INSTITUTE OF PHYSICS PUBLISHING NANOTECHNOLOGY
Nanotechnology **18** (2007) 035206 (4pp) doi:10.1088/0957-4484/18/3/035206

Effect of graphitic order on field emission stability of carbon nanotubes

Vijaya Kumar Kayastha, Benjamin Ulmen and Yoke Khin Yap[1]

Department of Physics, Michigan Technological University, Houghton, MI 49931, USA

E-mail: ykyap@mtu.edu

Received 25 August 2006, in final form 19 October 2006
Published 3 January 2007
Online at stacks.iop.org/Nano/18/035206

Abstract
We observed current density (J) dependent degradation in field emission current from multiwalled carbon nanotubes (MWCNTs). These degradations are recoverable and can be explained by emission current-induced dislocations along the MWCNTs. MWCNTs grown by thermal chemical vapour deposition (CVD) can emit stable current continuously for at least 1200 min with upper current density limits of ~0.5 mA cm^{-2}. In contrast, this upper limit is <40 μA cm^{-2} for nanotubes grown by plasma-enhanced CVD (PECVD), although higher J is possible with relatively shorter stability duration. High-resolution transmission electron microscopy and Raman spectroscopy indicate higher graphitic order of the thermal CVD grown MWCNTs as compared to PECVD grown MWCNTs. Our study suggests that graphitic order affects their upper performance limits of long-term emission stability, although the effects from adsorbates cannot be completely ignored. These results indicate that field emission cannot be considered as an ideal quantum tunnelling process. The effect of electron transport along CNTs before electron tunnelling must be considered.

1. Introduction

Carbon nanotubes (CNTs) are known to have excellent properties for electron field emission [1, 2]. Their high aspect ratio enables large electric field enhancement at their tips and initiates electron emission at moderate applied electric fields. Various CNTs have been tested in the past ten years. However, reliable commercial products including flat panel displays have not been demonstrated [3]. One of the main reasons is the lack of long-term emission stability. The fundamental factors that contribute to the emission stability have not been well studied. Most published works have focused on demonstrating the low emission threshold fields of CNTs [1–6], the electric field shielding effects [4], the device architecture [5], and the failure of CNTs after excessive current emission [6]. Furthermore, field emission has been considered as an ideal quantum tunnelling process. There are effects from the electron transport along CNTs that must be considered. Here, we start to scrutinize the basic mechanism that could help to resolve these long-standing issues. We show that the process of electron transport along CNTs is crucial for stable electron emission.

We anticipate that electron transport along CNTs will affect the field emission properties. Experiments were thus conducted to evaluate emission stability of various types of multiwalled CNTs (MWCNTs) grown by plasma-enhanced chemical vapour deposition (PECVD) and thermal CVD. CVD techniques have the advantage of enabling direct growth of patterned CNTs on substrates for device fabrication. We found that CNTs grown by thermal CVD exhibit far better emission current stability than those grown by PECVD. This is explained by the difference in their structural and graphitic orders detected by both electron microscopy and Raman spectroscopy. The upper performance limits of these CNTs were also evaluated. A model is proposed to represent the practical process of electron emission from CNTs, with the consideration of electron transport along CNTs, prior to the quantum tunnelling process.

2. Experimental details

MWCNT films were grown into circular areas of 0.385 cm^2 (diameter = 7 mm) on low resistance Si substrates (resistivity

[1] Author to whom any correspondence should be addressed.

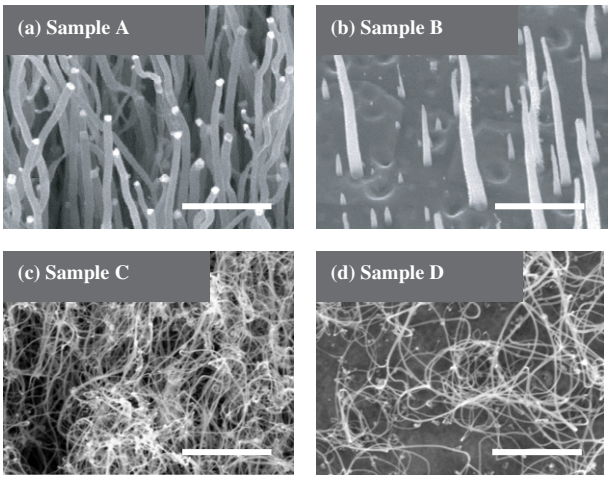

Figure 1. (a) High and (b) low density MWCNTs grown by PECVD. (c) High and (d) low density MWCNTs grown by thermal CVD. The scale bar is 1 μm.

$= 1\ \Omega\ \mathrm{cm}^{-1}$) by PECVD [7] and thermal CVD [8, 9]. Two types of MWCNT films were prepared by each technique (figure 1). We denote high and low density samples grown by PECVD as samples A and B, while those grown by thermal CVD as samples C and D respectively. The density of the PECVD MWCNTs was controlled by adjusting catalyst film thickness and the plasma configuration [7], while the density of MWCNTs grown by thermal CVD was controlled by adjusting the flow rate of NH_3 buffer gas [9]. All field emission measurements were conducted in a hanging planar diode configuration at a base pressure of 1.0×10^{-7} Torr [10]. The gap between the two electrodes was made relatively large (i.e. $1700 \pm 10\ \mu$m) without using a spacer to prevent possible arcing and surface tracking discharges between the electrodes. The effective distance from the sample surface to the anode was $\sim$1000 μm. All samples underwent conditioning by applying different levels of emission current-induced heating for 1200 min to remove adsorbates from the tip of the field emitters. Emission stability tests were then conducted for 1200 min at different initial current densities (J_0). Current density was defined as the average emission current per unit area of the sample. It was calculated by dividing the collected current by the growth area of the sample (0.385 cm^2). All samples were characterized by using a field emission scanning electron microscope (Hitachi S-4700), a high resolution transmission electron microscope (Hitachi HF-2000 FE, accelerating voltage: 200 kV), and a Raman spectrometer (Renishaw 100 confocal microscope) with a HeNe (632.8 nm) excitation laser ($\sim$30 mW) at typical probing areas of $\sim 2\ \mu\mathrm{m}^2$.

3. Results and discussion

Figure 2(a) shows emission stability for sample A at $J_0 = 200\ \mu\mathrm{A\ cm}^{-2}$. As shown, the emission current started to degrade immediately but stabilized after 400 min at a current density $J = 35\ \mu\mathrm{A\ cm}^{-2}$. Some current spikes are also detected after around 600 min. Figure 2(b) shows the current stability of sample B which shows similar degradation. This sample was first tested with $J_0 = 350\ \mu\mathrm{A\ cm}^{-2}$ and eventually stabilized at $J = 40\ \mu\mathrm{A\ cm}^{-2}$ (curve 1). We found that J_0 can be recovered when the sample was retested after switching off the applied electric field. Similar degradation was observed in the beginning and eventually stabilized at $J = 40\ \mu\mathrm{A\ cm}^{-2}$ (curve not shown). These results indicate that sample B is capable of stable emission if $J \leqslant 40\ \mu\mathrm{A\ cm}^{-2}$. This is confirmed by testing this sample at $J_0 = 25\ \mu\mathrm{A\ cm}^{-2}$ (curve 2). As shown, the emitted current is stable for 1200 min without degradation.

Figure 2(c) shows the stability test curves for sample C at different J_0. At $J_0 = 250\ \mu\mathrm{A\ cm}^{-2}$ (curve 1), there was a rise in emission current in the first 100 min. This current density then returned to J_0 after 540 min and was stable up to the tested duration of 1200 min. For $J_0 = 500\ \mu\mathrm{A\ cm}^{-2}$ (curve 2), there was a slow degradation of current for the first 900 min and then it became stable at a level of $450\ \mu\mathrm{A\ cm}^{-2}$. For $J_0 = 1\ \mathrm{mA\ cm}^{-2}$ (curve 3), the current dropped faster in the first 300 min and then became stable at $550\ \mu\mathrm{A\ cm}^{-2}$ up to the tested duration of 1200 min. A similar phenomenon was detected for sample D, as shown in figure 2(d). The emitted current is relatively stable when tested at $J_0 = 250\ \mu\mathrm{A\ cm}^{-2}$ (curve 1). The emitted current briefly degraded to $450\ \mu\mathrm{A\ cm}^{-2}$ when tested with $J_0 = 500\ \mu\mathrm{A\ cm}^{-2}$ (curve 2). This sample was then tested for $J_0 = 1\ \mathrm{mA\ cm}^{-2}$ (curve 3). The emitted current dropped continuously for the first 660 min and then became stable at $450\ \mu\mathrm{A\ cm}^{-2}$. These results show that MWCNTs grown by thermal CVD are stable electron emitters up to an upper current density limit of 450–550 $\mu\mathrm{A\ cm}^{-2}$. This upper limit is significantly higher than that for the PECVD MWCNTs discussed earlier.

In samples A and B, electrons are expected to emit near the tips of the nanotubes since higher electric field strengths are focused at the tips of these vertically aligned nanotubes. For long and random nanotubes in samples C and D, it is believed that electrons will be emitted from their tips as they were induced to align in the direction of the applied electric fields [11, 12]. In this case, the tips will be extended closer to the top electrode and gain higher field enhancement. However, we cannot completely ignore the possibility of electron emission from other parts of the nanotubes.

Figure 3 shows the emission current density (J) versus applied electric field (E) curves for these samples. The threshold electric fields E_{th} (applied electric field required to emit electrons at a level of $J = 1\ \mu\mathrm{A\ cm}^{-2}$) for samples A, B, C, and D were found to be 3.7, 2.4, 1.3 and 1.6 V $\mu\mathrm{m}^{-1}$ respectively. The lower E_{th} between samples A and B, and between samples C and D is due to optimum nanotube density (i.e. the minimum shielding effect) [4] and the difference in aspect ratio. Comparing the films grown by the two different techniques, clearly samples C and D have lower E_{th} than samples A and B. One factor contributing to this is the high field enhancement factors ($\beta \sim h/r$, h is the length and r is the tip radius of CNTs) of the longer and thinner thermal CVD MWCNTs, which can enhance the tunnelling of electrons. This is consistent with the Fowler–Nordheim (FN) relation, $J = A\beta^2 E^2 \exp(-B\Phi^{3/2}/\beta E)$ [13], where A, B are constants, E is the applied electric field in $\mathrm{V\ cm}^{-1}$, and Φ is the work function in eV. A larger β value will lead to larger J at a

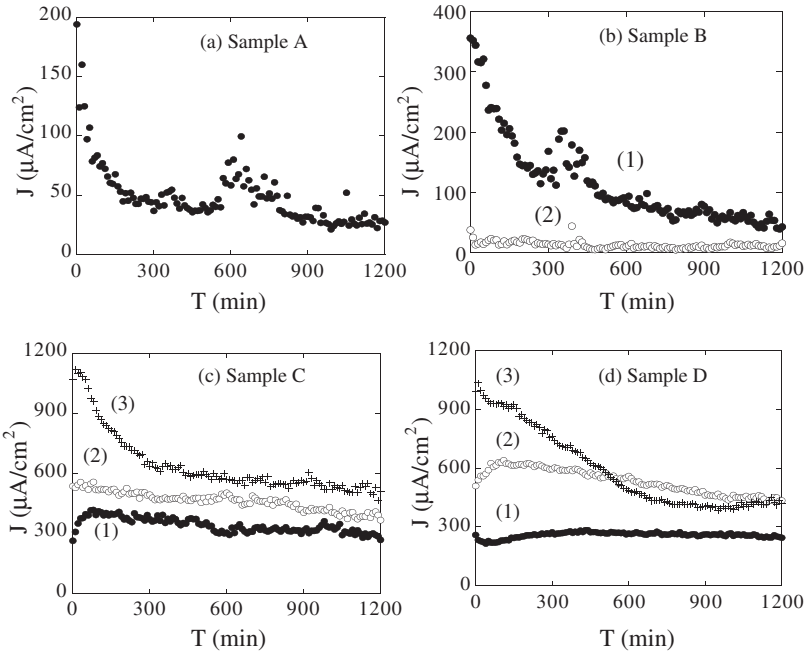

Figure 2. Emission current density (J) as a function of time (T) for sample (a) A, (b) B, (c) C, and (d) D at various initial current densities.

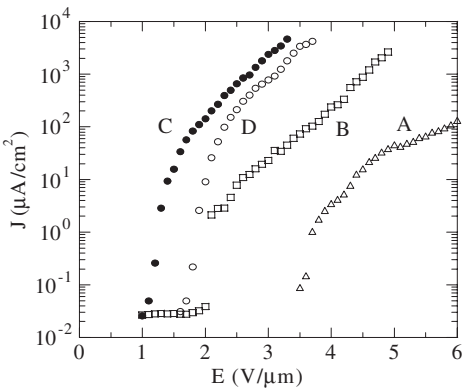

Figure 3. Emission current density (J) as a function of applied electric field (E) for samples A, B, C, and D.

particular E and Φ. The FN relation is sufficient to describe these transient J–E plots (figure 3) but cannot explain the stability degradation (figure 2).

There are two observations which require further explanation: What has caused the emission degradation? Why do the thermal CVD grown MWCNTs have higher upper limits of stable emission? Several mechanisms have been proposed to explain the degradation of field emission from CNTs. First, bombardment of ionic residual gas on CNTs as generated by the emitted electrons may damage the structure of the CNTs [14]. Secondly, the peeling of CNTs from the substrates could cause sudden current decay and arcing [15]. However, the degradation due to these factors is unrecoverable. So, these phenomena cannot explain our observations of recoverable degradations. Furthermore, no morphology changes were detected from our samples after the degradation tests as examined by electron microscopy. Other factors such as length, diameter and density of the CNTs will determine β, E_{th}, and the screening effect on these samples. There is no evidence or mechanisms showing that these factors will change the emission stability once the CNTs have start emitting. On the other hand, adsorbates are known to cause noise and flickering in the emission current [16], as also observed in our case before conditioning. Noisy emission current with relatively low threshold fields were observed during the first few cycles of I–V tests (conditioning). Stable I–V curves were then reproduced prior to our stability tests discussed earlier. This is explained by the evaporation of the adsorbates by Joule heating during field emission [16, 17]. However, we cannot completely ignore the possibility of residual adsorbates in our results as discussed later.

Since the degradation is current density dependent, we think that it is due to some type of current-induced dislocations that could work as electrons traps. These dislocations generated along the nanotubes will reduce the current that is delivered to the nanotube tips, prior to the field emission process. Furthermore, the dislocation occurs only above a certain threshold of current density which depends upon the graphitic order of the nanotubes. This mechanism is analogous to colour centres commonly detected in optical materials [18], where photons are absorbed by dislocations that were induced by intensive laser irradiance. These colour centres will not be created with low power lasers. A hypothetical model for this analogue is described as follows. In figure 4(a), the ideal condition of electron field emission is illustrated. In this case, only quantum tunnelling at the tip of the cathode to the anode is considered. Figure 4(b) represents the practical condition where the intrinsic impedance (Z_{in}, can be resistance, capacitance, inductance, and/or combinations of these) of the CNT is included, which causes Joule heating that has been experimentally confirmed [17]. In figure 4(c), we include a current-induced impedance, $Z(J)$ that represents

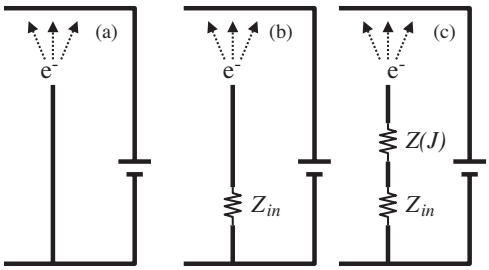

Figure 4. Schematic representation of one CNT at (a) ideal field emission, (b) practical field emission with intrinsic impedance (Z_{in}), and (c) practical field emission with Z_{in} and current-induced impedance, $Z(J)$.

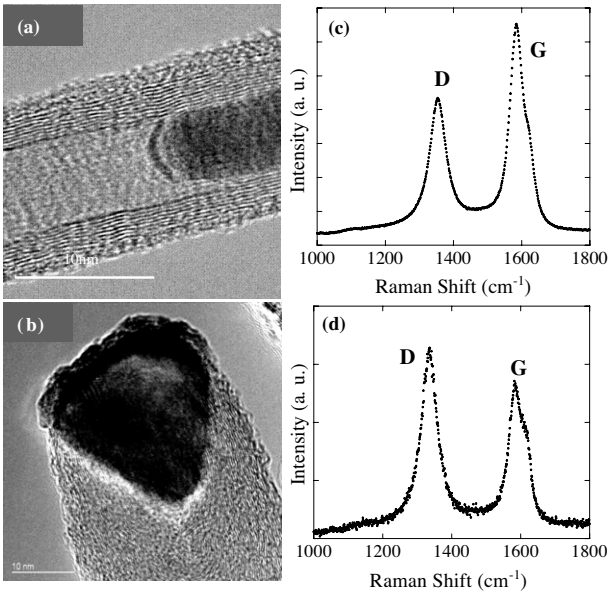

Figure 5. TEM images of MWCNTs grown by (a) thermal CVD, and (b) PECVD. The scale bar is 10 nm. Raman spectra from MWCNT films grown by (c) thermal CVD and (d) PECVD.

the current-induced dislocation that we proposed here. Future investigation is required to further understand the nature of these dislocations. On the other hand, Joule heating will generate thermal energy that could help to recover these dislocations when the stimulant (current flows) is removed. This explains the recovery of the emission properties after turning off the applied electric fields.

We attempt to explain the reason for the higher performance limits of the thermal CVD grown MWCNTs. Since all samples were tested in the same system and vacuum condition, the difference in performance should be related to their intrinsic structural properties. Transmission electron microscopy (TEM) shows that thermal CVD tubes (figure 5(a)) have better structural order than PECVD tubes (figure 5(b)). This is consistent with the Raman spectra, where the disorder-induced D-peak for PECVD tubes is stronger in intensity than the graphitic G-peak (figure 5(d)). Apparently, thermal CVD grown MWCNTs with higher graphitic order (figure 5(c)) are more resistant to current-induced dislocation and thus offer higher performance limits for stable electron field emission. In addition, less adsorbates may have been deposited on the thermal CVD grown MWCNTs due to the lower number of defective sites along the tubular structures. This could also contribute to the higher performance limits of these MWCNTs. There could be a relation between these adsorbates and the dislocation sites, which will require further investigation in the future.

4. Conclusions

In summary, we detected current density dependent degradation of emission current from MWCNTs. This is explained by the current-induced dislocation and electron trapping effects. There is an upper current density limit below which, stable electron emission can occur and above which, degradation occurs. These effects are more significant for MWCNTs that have lower graphitic orders. Our results indicate that field emission cannot be considered as an ideal quantum tunnelling process. The effect of electron transport along CNTs before electron tunnelling must be considered.

Acknowledgments

YKY acknowledges support from the Michigan Tech Research Excellence Fund, the Department of Army (W911NF-04-1-0029, through the City College of New York) and the Center for Nanophase Materials Sciences (CNMS) at Oak Ridge National Laboratory.

References

[1] de Heer W A, Châtelain A and Ugarte D 1995 *Science* **270** 1179
[2] Collins P G and Zettl A 1996 *Appl. Phys. Lett.* **69** 1969
[3] Choi W B, Chung D S, Kim H Y, Jin Y W, Han I T, Lee Y H, Jung J E, Lee N S, Park G S and Kim J M 1999 *Appl. Phys. Lett.* **75** 3129
[4] Nilsson L, Groening O, Emmenegger C, Kuettel O, Schaller E, Schlapbach L, Kind H, Bonard J M and Kern K 2000 *Appl. Phys. Lett.* **76** 2071
[5] Han I T, Kim H J, Park Y, Lee N, Jang J E, Kim J W, Jung J E and Kim J M 2002 *Appl. Phys. Lett.* **81** 2070
[6] Bonard J M, Klinke C, Dean K A and Coll B F 2003 *Phy. Rev.* B **67** 115406
[7] Menda J, Ulmen B, Vanga L K, Kayastha V, Yap Y K, Pan Z, Ivanov I N, Puretzky A A and Geohegan D B 2005 *Appl. Phys. Lett.* **87** 173106
[8] Kayastha V, Yap Y K, Pan Z, Ivanov I N, Puretzky A A and Geohegan D B 2005 *Appl. Phys. Lett.* **86** 253105
[9] Kayastha V, Yap Y K, Dimovski S and Gogotsi Y 2004 *Appl. Phys. Lett.* **85** 3265
[10] Ulmen B, Kayastha V, DeConinck A, Wang J and Yap Y K 2006 *Diamond Relat. Mater.* **15** 212
[11] Wei Y, Xie C, Dean K A and Coll B F 2001 *Appl. Phys. Lett.* **79** 4527
[12] Wang Z L, Gao R P, Heer W A D and Poncharal P 2002 *Appl. Phys. Lett.* **80** 856
[13] Fowler R H and Northeim L 1928 *Proc. R. Soc.* A **119** 173
[14] Hainfeld J F 1977 *Scanning Electron Microsc.* **1** 591
[15] Cheng Y and Zhou O 2003 *C. R. Physique* **4** 1021
[16] Semet V, Binh V T, Vincent P, Guillot D, Teo K B K, Chhowalla M, Amaratunga G A J, Milne W I, Legagneux P and Pribat D 2002 *Appl. Phys. Lett.* **81** 343
[17] Purcell S T, Vincent P, Journet C and Binh V T 2002 *Phys. Rev. Lett.* **88** 105502
[18] Tsai T E, Williams G M and Friebele E J 1997 *Opt. Lett.* **22** 224